

1 **Late Cretaceous (99-69 Ma) basaltic intraplate volcanism on and around**  
2 **Zealandia: Tracing upper mantle geodynamics from Hikurangi Plateau**  
3 **collision to Gondwana breakup**

4

5 K. Hoernle<sup>1,2</sup>, C. Timm<sup>1,3</sup>, F. Hauff<sup>1</sup>, V. Tappenden<sup>4</sup>, R. Werner<sup>1</sup>, E. M. Jolis<sup>1</sup>, N. Mortimer<sup>5</sup>,  
6 S. Weaver<sup>4</sup>, F. Riefstahl<sup>6</sup>, K. Gohl<sup>6</sup>

7

8 <sup>1</sup>GEOMAR Helmholtz Center for Ocean Research Kiel, 24148 Kiel, Germany

9 <sup>2</sup>Kiel University, Institute of Geosciences, 24118 Kiel, Germany

10 <sup>3</sup>GNS Science, Lower Hutt 5040, New Zealand

11 <sup>4</sup>Canterbury University, Christchurch, New Zealand

12 <sup>5</sup>GNS Science, Dunedin 9054, New Zealand

13 <sup>6</sup>Alfred Wegener Institute Helmholtz Center for Polar and Marine Research, 27568

14 Bremerhaven, Germany

15

16

17 **Abstract**

18 Collision of a young, buoyant plateau fragment with an active continental margin can lead to  
19 subduction cessation, but can it also trigger continental breakup? It has been postulated that  
20 the collision of the Hikurangi Plateau with the Gondwana margin at ~110 Ma ago, caused  
21 subduction to cease, large-scale extension and ultimately breakoff of the Zealandia micro-  
22 continent from West Antarctica through seafloor spreading starting at circa 90 Ma. Here we  
23 report new geochemical (major and trace element and Sr-Nd-Pb-Hf isotope) data for Late  
24 Cretaceous (99-69Ma) volcanism from Zealandia. Four geographically-separated provinces  
25 of intraplate magmatism formed during this time interval: 1) Hikurangi Seamount Province

26 (99-86 Ma), 2) Marlborough Igneous Province (98-94 Ma), 3) Westland Igneous Province  
27 (92-69 Ma), and 4) Eastern Chatham Igneous Province (86-79 Ma). Each of the intraplate  
28 provinces forms binary mixing arrays on incompatible-element and isotope ratio plots  
29 between HIMU (requiring long-term elevated  $\mu = {}^{238}\text{U}/{}^{204}\text{Pb}$ ) and either a depleted (MORB-  
30 source) upper mantle (DM) component or enriched continental crustal (EM) type component  
31 (located in the crust and/or upper mantle) or a mixture of both. St. Helena end member  
32 HIMU is the common component to all four provinces. Considering the uniformity in  
33 composition of the HIMU end member despite the type of lithosphere (continental, oceanic,  
34 oceanic plateau) beneath the igneous provinces, we attribute this component to a  
35 sublithospheric source, located beneath all volcanic provinces, and thus most likely a mantle  
36 plume. We propose that the plume rose beneath the active Gondwana margin and flowed  
37 along the subducting lithosphere beneath the Hikurangi Plateau and neighboring seafloor and  
38 through slab tears/windows beneath the Gondwana (later to become Zealandia) continental  
39 lithosphere. We conclude that both plateau collision, resulting in subduction cessation, and  
40 the opening of slab windows, allowing hot asthenosphere and plume material to upwell to  
41 shallow depths, were important in causing the breakup of Zealandia from West Antarctica.

42

43 **Key Words:** Zealandia continental breakup; Hikurangi Plateau collision; Gondwana  
44 subduction; major & trace element & isotope geochemistry; St. Helena HIMU mantle end  
45 member; mantle plume.

46

## 47 1. Introduction

48 A fundamental question in the Earth Sciences is what triggers continental breakup (e.g.  
49 Sleep, 1971; Condie, 2016). Many rifted margins are characterized by up to 15 km of  
50 underplated mafic crust and submarine seaward-dipping reflectors, which reflect subaerially-

51 erupted basaltic volcanism tilted during subsidence (e.g. Condie, 2016). They are generally  
52 associated with flood basalt events (e.g. Menzies et al., 2002) formed during the initial (or  
53 plume head) stage of a mantle plume (Richards et al., 1989). It is proposed that large plume  
54 heads (up to 2000 km in diameter) impinge on the base of the lithosphere, causing  
55 lithospheric mantle erosion and extension, both of which result in lithospheric thinning and  
56 isostatic uplift, rifting and eventually seafloor spreading.

57 Far-field extensional plate tectonic forces are believed to govern the formation of non-  
58 volcanic margins (Geoffroy, 2005). At some stage in their development, super continents are  
59 surrounded by subduction zones. Rollback of the subducting slab along much of this  
60 subduction network can lead to internal extension, resulting in continental breakup.  
61 Progressive extension of cool, sediment-poor continental lithosphere far from a mantle  
62 plume, for example the Iberian margin, has been proposed as a mechanism for generating  
63 non-volcanic margins (Reston, 2007). Propagation of spreading centers, as is presently  
64 occurring in the Woodlark Basin where spreading is propagating into and beginning to split  
65 Papua New Guinea, provides another potential mechanism for causing continental breakup.  
66 Alternatively, it has also been proposed that subduction of a spreading center or other change  
67 in plate boundary forces can lead to continental breakup (e.g. Bradshaw, 1989).

68 Here we investigate one of the late breakup phases of the Gondwana supercontinent: One  
69 of the most enigmatic continental breakup events in recent Earth history. This breakup event  
70 resulted in the separation of pieces of the present Zealandia micro-continent from Marie Byrd  
71 Land, West Antarctica (Mortimer et al., 2017). Proposed models to explain the breakup of  
72 Zealandia from Antarctica include: 1) collision of the Pacific-Phoenix spreading center with  
73 the Gondwana active margin (Bradshaw, 1989; Luyendyk, 1995; Storey et al., 1999; Tulloch  
74 et al., 2009), 2) impingement of a mantle plume head at the base of the Gondwana margin  
75 lithosphere at what is now Marie Byrd, Antarctica (Weaver et al., 1994; Storey et al., 1999),

76 3) collision of the Hikurangi Plateau with the Gondwana active margin (now the Chatham  
77 Rise) clogging the subduction system (e.g., Sutherland and Hollis, 2000; Davy et al., 2008;  
78 Hoernle et al., 2010; Reyners et al., 2011; Davy, 2014; Mortimer et al., 2019). A variation of  
79 model 3 involves normal faulting in the overlying basement along a SW continuation of the  
80 subducted western Wishbone Ridge (Mortimer et al., 2006). In most recent models, the  
81 collision of the Hikurangi Plateau, one of the three major fragments of the Ontong Java-  
82 Manihiki-Hikurangi superplateau (e.g., Taylor, 2006; Davey et al., 2008; Hochmuth et al.,  
83 2015), with the Gondwana active margin is invoked as the initial trigger of this breakup.  
84 Based on relocated seismicity, Reyners et al. (2017) postulate that the Hikurangi Plateau is  
85 underplated beneath much of the South Island of New Zealand terminating at the southern  
86 portion of the South Island. Major open questions include: What happens in the upper mantle  
87 during collision of an igneous oceanic plateau or Large Igneous Province (LIP) with an active  
88 continental margin? What role does such a collisional event play in causing continental  
89 breakup? Did a mantle plume play a role in triggering the breakup?

90 Here we will evaluate these questions using age and geochemical data from four different  
91 intraplate magmatic provinces (Fig. 1, 2): Hikurangi Igneous Seamount Province (99-84 Ma;  
92 Hoernle et al., 2010) - consisting of alkalic seamounts on the Hikurangi Plateau, formed after  
93 collision of Hikurangi Plateau with the Gondwana margin, 2) Marlborough Igneous Province  
94 (98-94 Ma; Baker et al., 1994; Tappenden, 2003; McCoy-West et al., 2010; Mortimer et al.,  
95 2019) - alkalic volcanism on the northern South Island east of the South Alpine Fault,  
96 including Lookout, Gridiron, Mandamus and Tapuaenuku Igneous complexes, 3) Westland  
97 Igneous Province (92-69 Ma; van der Meer et al., 2016; van der Meer et al., 2017; Mortimer  
98 et al., 2019) - tholeiitic to lamprophyric Westland and Hohonu dikes on the northern South  
99 Island west of the Alpine Fault, and 4) East Chatham Volcanic Province (86-78 Ma; Panter et  
100 al., 2006; Homrighausen et al., 2018; Mortimer et al., 2019) - transitional to alkalic lavas on

Chatham Island and seamounts on the East Chatham Rise and the surrounding seafloor. We use the temporal evolution of these four intraplate volcanic provinces to reconstruct processes occurring within the subducted lithosphere and within the mantle beneath the former Zealandia active margin until breakup, including the early history of seafloor spreading between Zealandia and West Antarctica.

## **2. Samples and Analytical Methods**

For the present study, volcanic rocks were dredged from five submerged volcanoes on the eastern Chatham Rise, one from DSDP Site 595, 30 locations from the Marlborough volcanic province (Mandamus Igneous complex, Lookout and Gridion volcanics), 10 locations from the Westland province (Hohonu Dikes), 28 locations from the Mount Somers volcanic group (including two sites from the Torlesse metasediments) (Figure 1). At all sites discussed here, the angular shape of the rocks, freshly broken surfaces, and the homogeneity of rock types indicate an in-situ (not ice-rafted) origin for the dredged rocks. Sampling localities are summarized in Supplementary Table 1.

Analytical methods are reported in Supplementary File 1.

## **3. Results**

We present new geochemical (major and trace element and Sr-Nd-Hf-Pb isotope; Supplementary Tables 1 & 2) data on volcanism from the Marlborough, Westland and Mt. Somers Igneous Provinces and seamounts on and near the eastern Chatham Rise, collected by dredging on the R/V SONNE SO168 and SO246 expeditions (Table 1).  $^{40}\text{Ar}/^{39}\text{Ar}$  ages and additional background information for many of the samples are reported in Mortimer et al. (2019) and Homrighausen et al. (2018). We combine our new results with those from published studies (Hoernle et al., 2006; Mortimer et al., 2006; Panter et al., 2006; McCoy-

126 West et al., 2010; Timm et al., 2010; Homrighausen et al., 2018; van der Meer et al., 2010,  
127 2016) to reconstruct the evolution of intraplate volcanism on and around Zealandia from  
128 ~100-70 Ma.

129 Alteration has affected many of these samples, in particular considering their Late  
130 Cretaceous age and the submarine history of some of the samples. With decreasing MgO,  
131 both SiO<sub>2</sub> and Al<sub>2</sub>O<sub>3</sub> (until ~5wt.% for East Chatham and Mt. Somers samples) roughly  
132 increase, whereas CaO (until ~7wt.% MgO) and FeO<sup>t</sup> (total iron until ~5wt.% MgO) remain  
133 roughly constant and then begin to decrease. TiO<sub>2</sub> and P<sub>2</sub>O<sub>5</sub> increase initially and begin to  
134 decrease at MgO ~5wt.% (except for Westland samples). The observed trends are consistent  
135 with fractionation of the observed major phenocryst phases in the samples in the sequence  
136 olivine, clinopyroxene, Fe-Ti oxides, ± plagioclase and apatite (Tappenden, 2003; Panter et  
137 al., 2006; McCoy-West et al., 2010; van der Meer et al., 2010, 2016).

138 Considering that the alkalis have been mobilized in many samples, we use the Nb/Y vs.  
139 Zr/Ti plot (after Pearce, 1996) to classify the rocks (Fig. 3a), which relies on ratios of  
140 immobile incompatible elements. The intraplate samples range from tholeiites (Southern  
141 Volcanics from Chatham Island) to alkali basalts (most samples) through alkali rhyolites to  
142 foidites through phonolites (primarily Westland rocks), whereas the Mt. Somers rocks range  
143 from andesite to dacite - rhyolite - trachyte. On the Nb/Yb vs. Th/Yb and TiO<sub>2</sub>/Yb diagrams  
144 (Fig. 3b,c) after Pearce (2008), most of the intraplate igneous rocks have alkalic ocean-island  
145 basalt (OIB) affinities. The Hikurangi, Marlborough, Westland and East Chatham province  
146 igneous rocks form arrays that extend from the OIB domain to lower Nb/Yb ratios with some  
147 samples plotting within the mantle array in the direction of mid-ocean-ridge basalts  
148 (MORBs) and other samples plotting above the mantle array in the volcanic arc and crustal  
149 field. The Mt. Somers volcanic rocks with subduction and/or continental geochemical  
150 affinities (Tappenden, 2003) plot well above the mantle array clustering around typical

Torlesse metasediments from Canterbury. On multi-element diagrams showing incompatible elements for the freshest samples with highest MgO and most radiogenic Pb isotope ratios, to minimize the effects of alteration, differentiation and crustal assimilation (Fig. 4), the Hikurangi, Marlborough, Westland and East Chatham volcanic rocks display positive Nb and Ta anomalies and negative K and Pb anomalies characteristics of OIB, whereas the Mt. Somers rocks display clear negative Nb, Ta and positive K, Pb anomalies characteristic of subduction-related volcanism and crustal rocks.

Isotope correlation diagrams can be used to evaluate the sources from which igneous rocks are derived (Fig. 5). On the uranogenic Pb ( $^{206}\text{Pb}/^{204}\text{Pb}$  vs  $^{207}\text{Pb}/^{204}\text{Pb}$ ) isotope diagram (Fig. 5A), the 99-69 Ma intraplate igneous rocks form a broad array with positive slope between St. Helena end member HIMU (high time-integrated  $\mu = ^{206}\text{Pb}/^{204}\text{Pb}$ ) and the low- $\mu$  enriched mantle (EM), represented by Mt. Somers and Hikurangi Plateau basement rocks. On the  $^{206}\text{Pb}/^{204}\text{Pb}$  vs.  $^{143}\text{Nd}/^{144}\text{Nd}$  and  $^{87}\text{Sr}/^{86}\text{Sr}$  isotope diagrams (Fig. 5B,C), the four intraplate provinces form binary arrays that converge on the St. Helena HIMU field at radiogenic Pb isotope ratios. The Hikurangi Province samples form a roughly horizontal array, extending to the Hikurangi Plateau basement at the end with unradiogenic Pb isotope ratios. The Westland samples form a crude negatively-sloped array trending towards MORB at its unradiogenic end, and the Marlborough and East Chatham provinces form concave-down hyperbolas, ending near the Mt. Somers samples at their ends with unradiogenic Pb isotope ratios.

#### 4. Discussion

During much of the Mesozoic, present-day Zealandia formed part of the southern Gondwana active continental margin, located adjacent to what is presently Marie Byrd Land, West Antarctica. At ~120-125 Ma ago, the Ontong Java Nui, the largest known Phanerozoic volcanic event on Earth, formed in the western Pacific, covering more than 1% of Earth's

surface (Taylor, 2006; Davy et al., 2008; Hoernle et al., 2010; Timm et al., 2011; Hochmuth et al., 2015). Shortly after its formation, this super plateau broke apart into at least three major plateau fragments: 1) Ontong Java, 2) Manihiki and 3) Hikurangi. The Hikurangi and Manihiki Plateaus rifted apart between 115-120 Ma along the Osbourn Trough spreading system (Mortimer et al., 2006; Hochmuth et al., 2015). Thereafter the Hikurangi Plateau drifted southwards from the Manihiki Plateau until it collided with the Gondwana active margin at ~110-105 Ma (e.g. Bradshaw, 1989; Mortimer et al., 2006; Davy et al., 2008). The buoyant (then ~15-20 Ma old) Hikurangi Plateau clogged the Gondwana subduction zone, causing cessation of subduction along the northern edge of what is now the Chatham Rise (e.g., Sutherland and Hollis, 2000; Davy et al., 2008; Reyners et al., 2011; Davy, 2014; Mortimer, 2019).

#### 4.1 Formation of four intraplate volcanic provinces after Hikurangi Plateau collision

Four different mafic intraplate volcanic provinces (~99-69 Ma) formed on Gondwana continental crust (now Zealandia), the Hikurangi Plateau and the surrounding seafloor shortly after the Hikurangi Plateau collided with the Gondwana margin. The four intraplate volcanic provinces form distinct binary arrays on trace element and isotope diagrams (Fig. 3-5) that converge on a common composition. Below we will first discuss the binary arrays formed by each volcanic province, and then the common component involved in all four of the provinces.

The oldest ages come from the Hikurangi and Marlborough Provinces. The seamounts on the Hikurangi Plateau record ages of 99-86 Ma (Hoernle et al., 2010). The seamounts have a distinct composition from the Hikurangi basement. The basement has an EM type trace element (relatively flat incompatible element patterns on multi-element diagrams) and Sr-Nd-Pb isotopic composition similar to the main plateau-building stage on Ontong Java formed by



201 the Kwaimbaita/Kroenke lavas (Hoernle et al., 2010). The dominant Kwaimbaita lavas  
202 represent differentiates of the mafic Kroenke lavas, which have identical Sr-Nd-Pb-Hf  
203 isotopic compositions. The Hikurangi seamounts, on the other hand, have more enriched  
204 incompatible element abundances and fractionated heavy rare earth elements, forming  
205 patterns with a negative slope on multi-element diagrams. The seamounts form an array on  
206 incompatible-element and isotope ratio diagrams, extending from the St. Helena HIMU end  
207 member field to the EM-type plateau basement field (Fig. 5). The array can most easily be  
208 explained by mixing of HIMU melts with EM melts from the Hikurangi Plateau basement or  
209 underlying lithosphere, overprinted with a similar composition during emplacement of the  
210 LIP. Although a HIMU-type component (but not with end member St. Helena type  
211 composition) has been found in the ~125 Ma Manihiki basement (Timm et al, 2011; Golowin  
212 et al. 2018), no evidence for the presence of a St. Helena type HIMU end member component  
213 has been found within the basement of the Hikurangi Plateau. The most radiogenic Manihiki  
214 basement lavas only have  $^{206}\text{Pb}/^{204}\text{Pb}_{\text{in}}$  of ~19.7 and both  $^{207}\text{Pb}/^{204}\text{Pb}_{\text{in}}$  and  $^{208}\text{Pb}/^{204}\text{Pb}_{\text{in}}$  are  
215 lower in the Manihiki basement lavas at a given  $^{206}\text{Pb}/^{204}\text{Pb}_{\text{in}}$  than in the Hikurangi Seamount  
216 lavas, indicating that this HIMU-like component has a different composition than St. Helena  
217 and Cook-Austral end member HIMU. Accordingly, it is unlikely that the St. Helena end  
218 member HIMU component in the Hikurangi seamount lavas was derived from the Hikurangi  
219 Plateau basement or lithospheric mantle overprinted by the melts forming the plateau  
220 basement. Since the Hikurangi Plateau is believed to have formed on young ocean crust near  
221 a spreading center (Hochmuth et al., 2015), the pre-existing lithosphere is also an unlikely  
222 source for the HIMU component. Therefore, we favor an asthenospheric source for the  
223 HIMU component in the Hikurangi seamount lavas.

224 The intraplate Marlborough Igneous Province (98-94 Ma; Baker et al., 1994; Tappenden,  
225 2003; McCoy-West et al., 2010; Mortimer et al., 2019) on the northern South Island and the

226 calc-alkaline, Mt. Somers volcanic rocks, located in the central South Island, were both  
227 located in the forearc of the Gondwana subduction zone, north (or trench-wards) of the 232-  
228 105 Ma Median Batholith (e.g., Tappenden, 2003; van der Meer et al., 2018). On  
229 incompatible-element and isotope ratio diagrams (Fig. 3, 5), the Marlborough intraplate rocks  
230 form an array from the St. Helena HIMU mantle end member towards an enriched  
231 composition, which has more radiogenic Sr and less radiogenic Nd, Hf and Pb isotope ratios  
232 than the HIMU end member. The Sr-Nd-Pb-Hf isotopic variations in the Marlborough  
233 igneous rocks could be explained by assimilation of up to ~25% crustal rocks, but generally  
234 <10%, from the Early Cretaceous Pahau terrane rocks (Tappenden, 2003; McCoy-West et al.,  
235 2010). We however do not see any clear correlations between indices of differentiation (e.g.  
236 SiO<sub>2</sub> or MgO) with Sr-Nd-Pb isotope ratios in our data (not shown), but rather each isotope  
237 ratio forms relatively flat trends on diagrams of isotope ratios versus an index of  
238 differentiation. Therefore, if these trends are caused by crustal assimilation, they are not  
239 coupled to differentiation, i.e. assimilation during fractional crystallization (AFC). Although  
240 oxygen isotopic disequilibrium between clinopyroxene cores and rims suggests phenocrysts  
241 interacted with meteoric water in shallow magma chambers (McCoy-West et al., 2010), this  
242 will not necessarily show up in radiogenic isotope systems, especially not for immobile  
243 elements such as Nd and Hf.

244 The calc-alkaline Mt. Somers rocks also have enriched isotopic compositions that could  
245 serve as the enriched end member for the Marlborough Province intraplate rocks. Due to low  
246 Pb concentrations and low Nd/Pb ratios, mixing of mafic Marlborough melts with Mt.  
247 Somers rocks would generate concave down mixing curves that can also explain the observed  
248 Marlborough array.

249 The calc-alkaline Mt. Somers volcanic rocks display typical incompatible-element  
250 characteristics of subduction zone volcanism, such as relative depletion in Nb, Ta and relative

251 enrichment in K and Pb, compared to other elements with similar degrees of incompatibility  
252 (Fig. 4). Tulloch et al. (2009) have argued that, because of their 96 Ma age, the Mt Somers  
253 lavas are actually intraplate continental tholeiites, indistinguishable from subduction-related  
254 suites on the basis of their whole rock chemistry. This remains an open issue. Whatever their  
255 origin, these incompatible-element characteristics are opposite to those of the intraplate  
256 Marlborough igneous rocks, which show relative enrichment in Nb, Ta and relative depletion  
257 in K and Pb. The major and trace element characteristics of the Mt. Somers rocks are  
258 consistent with the melts having been influenced by the mantle wedge of the Gondwana  
259 subduction zone, implying that the isotopic composition of the parental melts also represent  
260 those of the Gondwana mantle wedge (asthenosphere and lithosphere) located beneath the  
261 South Island in the mid Cretaceous. Although the mantle wedge could have an upper mantle  
262 type composition, represented by normal MORB, this is unlikely considering that marine  
263 sediments, as evidenced in the accreted forearc sequence, subducted beneath the Gondwana  
264 margin. Nevertheless, with the present database, it is not possible to distinguish the exact  
265 composition of the mantle-derived melts and the amount of crustal assimilation that has taken  
266 place. In conclusion, the Marlborough Province mixing array could be explained by  
267 interaction of HIMU mantle melts with the enriched Pahau terrane crustal rocks and/or  
268 potentially enriched (Mt. Somers-type) mantle wedge.

269     Although it has been argued that the source of the HIMU end member may have been  
270 located in the lithospheric portion of the mantle wedge, reflecting metasomatism by  
271 subduction-related silicate melts (e.g. Panter et al., 2006), we note that subduction-related  
272 rocks are characterized globally by Pb enrichment and low U/Pb ratios. They are also  
273 characterized by enrichment in other fluid mobile incompatible elements, as well as relative  
274 depletions in Nb and Ta. These characteristics are distinct from intraplate volcanic rocks, so  
275 it is not clear how a HIMU-type source could be created in the lithosphere above a

276 subducting slab. Furthermore, no HIMU-type melts have been found on the South Island with  
277 an age >98 Ma. Considering the longevity of subduction along the Gondwana margin, why  
278 would HIMU compositions suddenly start erupting at 98 Ma if they are formed in the  
279 subduction zone environment? For the aforementioned reasons, we do not favor a  
280 lithospheric mantle source for the Marlborough intraplate HIMU melts, but rather a deep,  
281 ancient source as will be discussed in more detail below.

282     After cessation of Marlborough volcanism at ~94 Ma, volcanism moved to the Westland  
283 Igneous Province, which includes northern and central Westland and the Hohonu mafic dikes  
284 (92-69 Ma; van der Meer et al., 2016; van der Meer et al., 2017; Mortimer et al., 2019). At  
285 the time of the Westland magmatism, this region was located south of the Median Batholith  
286 and thus in the back-arc region, hundreds of kilometers south of the Marlborough and Mt.  
287 Somers volcanic provinces. The basement beneath this province consists of an amalgamation  
288 of Cambrian to Ordovician volcanic arc, passive margin and forearc turbidite assemblages,  
289 which were collectively metamorphosed to greenschist facies in the late Ordovician and  
290 subsequently intruded by Mesozoic granites, making up 50% of the present basement (van  
291 der Meer et al., 2018). The mafic volcanic rocks were erupted in two distinct phases  
292 becoming younger to the south: 1) northern Westland and Hohonu dikes (~92-83 Ma), 2)  
293 central Westland dikes (~72-69 Ma) (van der Meer et al., 2016). This confirms a southern  
294 progression in intraplate volcanism on the overriding plate after cessation of subduction at  
295 ~100 Ma from the Marlborough Province to northern Westland/Hohonu to central and  
296 southern Westland. These volcanic rocks have OIB-type incompatible element abundances  
297 (Fig. 3,4), displaying relative Nb enrichment and K and Pb depletions (van der Meer et al.,  
298 2016; van der Meer et al., 2017). They also form a crude array on isotope diagrams between a  
299 HIMU-like component and a depleted upper mantle MORB source (Fig. 5b). The overall less  
300 radiogenic Pb isotope ratios for the Westland samples with the most radiogenic Pb

301 ( $^{206}\text{Pb}/^{204}\text{Pb}_{90\text{Ma}} \leq 19.4$ ) could reflect greater dilution of HIMU type mantle melts with  
302 depleted upper mantle  $\pm$  enriched mantle wedge material and/or crust in the mafic Westland  
303 igneous rocks.

304 Contemporaneous with the Westland and Hohonu magmatism, the Eastern Chatham  
305 Province, including the Chatham Islands and seamounts on the eastern Chatham Rise, were  
306 active from ~86-79 Ma (Panter et al., 2006; Mortimer et al., 2006; Mortimer et al., 2019).  
307 Two intraplate seamounts north of the easternmost Chatham Rise and east of the West  
308 Wishbone Ridge, located on the mid Cretaceous (98-92 Ma; Mortimer et al., 2019) Pacific  
309 ocean crust, have similar ages of 86 Ma (Chicken Seamount) and 81 Ma (Pukeko Seamount)  
310 to the East Chatham Rise volcanism (Homrighausen et al., 2018; Mortimer et al., 2019). The  
311 East Chatham rocks have incompatible element characteristics that extend from the OIB field  
312 to both subduction and EMORB-type compositions (Fig. 3). Chicken Seamount volcanic  
313 rocks have St. Helena end member composition with more radiogenic  $^{206}\text{Pb}/^{204}\text{Pb}_{90\text{Ma}}$  than all  
314 of the East Chatham Province intraplate volcanic rocks, including those from Chatham Island  
315 that also fall within the end member St. Helena HIMU compositional field (Panter et al.,  
316 2006; Homrighausen et al., 2018), overlapping with the Hikurangi and Marlborough rocks  
317 with the most radiogenic Pb on the isotopic diagrams (Fig. 5). The East Chatham isotope data  
318 can be explained by mixing HIMU mantle melts with low- $\mu$  components ranging from  
319 enriched Mt. Somers mantle wedge and/or crustal Takahe granite (Mortimer et al., 2006) type  
320 compositions to a normal MORB type composition.

321

#### 322 4.2 A common HIMU end member for the Late Cretaceous intraplate volcanism

323 Four different mafic intraplate volcanic provinces (99-69 Ma) formed on contiguous  
324 Gondwana continental crust (now Zealandia), the Hikurangi Plateau and the surrounding  
325 seafloor shortly after the Hikurangi Plateau collided with the Gondwana margin. The four

intraplate volcanic provinces form distinct arrays on trace element and isotope diagrams (Fig. 3-5). As discussed above, the low  $\mu$  end of the mixing arrays can be explained by interaction of a common HIMU type component with the widely differing types of overlying lithosphere and possibly also shallow asthenosphere. The Hikurangi seamounts formed on the oceanic Hikurangi Plateau after it was transported nearly 3000 km southwards from where it formed together with the Manihiki and possibly Ontong Java Plateaus at ~120 Ma on Late Jurassic or Early Cretaceous oceanic crust (Taylor, 2006; Davey et al., 2008; Hoernle et al., 2010; Timm et al., 2011; Hochmuth et al., 2015). The Westland, Marlborough and East Chatham volcanic provinces formed largely on different age and types of continental lithosphere, which overlay the subducting Pacific oceanic lithosphere. Several seamounts belonging to the East Chatham Province (e.g. Chicken and Pukeko seamounts) are, however, located on Cretaceous (~98-92 Ma; Mortimer et al., 2019) Pacific ocean crust. Despite the variation in the age and nature (oceanic crust and plateau versus continental crust) of the overlying lithosphere, the trace element and isotope ratios from each volcanic province form arrays that converge on a common end member (Fig. 5).

The common end member in the Late Cretaceous intraplate lavas has radiogenic Pb, relatively radiogenic Nd and Hf, and unradiogenic Sr isotope ratios, falling within the range of end member HIMU compositions from St. Helena, which has a similar isotopic composition to the Cook-Austral Islands, but with higher  $^{207}\text{Pb}/^{204}\text{Pb}$  at a given  $^{206}\text{Pb}/^{204}\text{Pb}$  isotope ratio (e.g. Chaffey et al., 1989; Hanyu et al., 2011; Nebel et al. 2013). The common end member is also characterized by enrichment of highly and moderately incompatible elements, and displays relative enrichment in Nb and Ta and relative depletion of K and Pb compared to elements with similar incompatibility (Fig. 4). Although the depletion in K and Pb have been used to argue for amphibole in the source of the Late Cretaceous New Zealand lavas and thus for a subcontinental lithospheric mantle source (SCLM; e.g. Panter et al.,

2008; McCoy-West et al., 2016; van der Meer et al., 2017), we note that the classic end member HIMU localities (St. Helena, Mangaia and Tubuaii Islands) with these trace element and isotopic characteristics were erupted on oceanic lithosphere and thus cannot be derived directly from subcontinental lithospheric mantle (SCLM). Although Archean and Early Proterozoic subcontinental lithospheric mantle (SCLM) can have HIMU type compositions, intraplate lavas not located on continental crust of this age could be derived from ocean crust or SCLM recycled through the lower mantle via subduction and mantle plumes (e.g., Hofmann and White, 1982; Weis et al., 2016; Homrighausen et al., 2018). The most compelling argument that the HIMU end member component is related to mantle plumes is that at both type localities (St. Helena and Cook-Austral) mantle plumes can be imaged beneath the hotspots to the base of the lower mantle (e.g. Montelli et al., 2006; French and Romanowicz, 2015).

A popular model for the formation of the HIMU component in Zealandia lavas invokes derivation from relatively young (no more than a few hundred million years old) metasomatized lithospheric mantle (e.g. Panter et al., 2006; McCoy-West et al., 2016; van der Meer et al., 2017). This model, however, is unrealistic for the common HIMU end member observed in the Late Cretaceous Zealandia/Hikurangi volcanic provinces, because 1.0-3.2 Ga are needed to form end member HIMU from St. Helena and the Cook-Austral Islands based on Pb isotope model ages (e.g. Hofmann, 1997; Hanyu et al. 2011; Nebel et al. 2013; Homrighausen et al., 2018). Numerical simulations of the source evolution and mixing relationships, on the other hand, suggest a minimum formation age for HIMU of 2.0-2.5 Ga (Kimura et al., 2016). In order to explain the negative  $\Delta^{33}\text{S}$  isotope ratios in olivines from Cook-Austral HIMU, it has been argued that the source has to be  $\geq 2.45$  Ga in age (Cabral et al., 2013). Although high  $^{206}\text{Pb}/^{204}\text{Pb}$  isotope ratios of end member HIMU can be produced by very high  $^{238}\text{U}/^{204}\text{Pb}$  ratios on the scale of a few hundred million years, high  $^{207}\text{Pb}/^{204}\text{Pb}$

376 cannot be generated in such a short time span in the present earth from recycled normal  
377 MORB type ocean crust or in the depleted upper mantle, because most of the  $^{235}\text{U}$  with a  
378 half-life of  $\sim 0.7$  Ga has decayed since Earth formation, such that in today's Earth there is  
379  $\sim 138$  times as much  $^{238}\text{U}$  as  $^{235}\text{U}$ .

380 Other problems also exist with the proposition that subduction-related melts  
381 metasomatized the overlying subcontinental lithospheric mantle (SCLM) to form the HIMU  
382 type compositions. First, there is no evidence that subduction ever occurred beneath the  
383 Hikurangi oceanic lithosphere, either before or after formation of the plateau, and beneath the  
384 lithosphere on which the Chicken and Pukeko seamounts are located. Furthermore,  
385 subduction zone melts generally have very low  $\mu$ , reflecting greater mobility of Pb in hydrous  
386 fluids and melts than U. To our knowledge, there is no evidence of HIMU type compositions  
387 having been formed in the Gondwana supra-subduction setting. Finally, metasomatism  
388 generally creates very heterogeneous sources, which is inconsistent with the convergence of  
389 the Cretaceous intraplate volcanism on a fairly narrow isotopic compositional range similar  
390 to that of St. Helena lavas. Instead, the uniform composition of the common HIMU  
391 component must be derived from a well-mixed sublithospheric source in the convecting  
392 mantle that could generate melts beneath oceanic (normal MOR type crust and oceanic  
393 plateau crust) and diverse continental lithosphere. In conclusion, we favor derivation of the  
394 HIMU end member from a deep homogeneous reservoir and that the different igneous  
395 provinces were fed by a mantle upwelling (plume) or upwellings (plumes) from this  
396 reservoir.

397 In contrast to the Late Cretaceous Volcanic Provinces, Cenozoic intraplate volcanism on  
398 Zealandia requires an end member with radiogenic  $^{206}\text{Pb}/^{204}\text{Pb}_{90\text{Ma}}$ , in some cases within the  
399 end member HIMU range, but with lower  $^{207}\text{Pb}/^{204}\text{Pb}_{90\text{Ma}}$  and slightly higher  $^{143}\text{Nd}/^{144}\text{Nd}_{90\text{Ma}}$   
400 (Fig. 5; Timm et al., 2010). Derivation of the Cenozoic intraplate volcanism from SCLM is



possible. The Gondwana SCLM is likely to have consisted of depleted upper mantle (DM) that was partially metasomatized by subduction zone fluids and melts containing a subducted sediment component (and thus EM type composition). Ascending Cretaceous HIMU melts would have overprinted the lithosphere forming SCLM representing a mixture of St. Helena HIMU with DM and EM type components. Mantle xenoliths from the southern South Island largely fall on an array between a Cretaceous-type HIMU end member and depleted (DM) and/or enriched (EM) type upper mantle on Pb isotope diagrams (Fig. 4c in McCoy-West et al., 2016). Nevertheless, many of the xenoliths have isotopic compositions shifted to the right of this mixing array, i.e. to more radiogenic  $^{206}\text{Pb}/^{204}\text{Pb}$ . These samples however have  $^{207}\text{Pb}/^{204}\text{Pb}$  lower than HIMU. The shift to the right of the HIMU - DM+EM mixing array can be explained by short-term (99-69 Ma) radiogenic ingrowth of mantle with elevated  $\mu$  ratios, since little  $^{235}\text{U}$  (which decays to  $^{207}\text{Pb}$ ) remains on Earth at the present. Such an ingrowth model could explain not only the composition of the xenoliths but also the greater heterogeneity in the Cenozoic lavas and the lower  $^{207}\text{Pb}/^{204}\text{Pb}$  (and slightly higher  $^{143}\text{Nd}/^{144}\text{Nd}$ ) at a given  $^{206}\text{Pb}/^{204}\text{Pb}$  than observed in the Cretaceous lavas.

Based on studies of dikes from Marie Byrd Land, Antarctica with  $^{40}\text{Ar}/^{39}\text{Ar}$  ages of  $107 \pm 5$  Ma, it has been proposed that a HIMU-type plume head beneath Marie Byrd Land may also have served as the trigger for the final phase of Gondwana breakup (Weaver et al., 1994; Storey et al., 1999). We note, however, that none of the dikes have classic HIMU trace element (lacking pronounced relative Nb and Ta enrichments and K and Pb depletions; Storey et al., 1999) or radiogenic Pb isotopic compositions (e.g.  $^{206}\text{Pb}/^{204}\text{Pb} > 20.5$ , as is the case for St. Helena, Tubuaii and Mangaia end member HIMU islands and the Late Cretaceous Zealandia, Hikurangi and nearby seafloor volcanism; e.g. Zindler and Hart, 1986). The Pb isotope ratios of the dikes ( $^{206}\text{Pb}/^{204}\text{Pb} = 18.74\text{--}19.02$ ,  $^{207}\text{Pb}/^{204}\text{Pb} = 15.61\text{--}15.63$  and  $^{208}\text{Pb}/^{204}\text{Pb} = 38.53\text{--}38.78$ ) are instead typical of Antarctic Peninsula crust (Fig. 7

426 in Storey et al., 1999), either reflecting extensive crustal assimilation or source contamination  
427 by subducted sediments with a similar composition to the Antarctic Peninsula crust.  
428 Furthermore, it was assumed that the Hikurangi Plateau was formed at the same time as the  
429 Antarctica dikes and to have a HIMU composition (Storey et al., 1999), we now know that  
430 the Hikurangi Plateau formed contemporaneous with the Ontong Java and Manihiki Plateaus,  
431 thousands of kilometers to the north of the Gondwana margin and that the basement has a  
432 EM (rather than HIMU) type composition similar to the Kwaimbaita/Kroenke lavas from  
433 Ontong Java (Taylor et al., 2006; Davies et al., 2008; Hoernle et al., 2010). Finally, the SE  
434 margin of Zealandia (the Campbell Plateau) and conjugate margin in Marie Byrd Land  
435 (Tulloch et al., 2019), Antarctica aren't volcanic type margins. Therefore, there is no  
436 compelling evidence for the emplacement of a HIMU type plume head beneath Marie Byrd  
437 Land at ~107 Ma; in contrast to the evidence for a HIMU plume(s) ascending beneath  
438 Zealandia and the Hikurangi Plateau between ~99-69 Ma.

439     Some evidence exists for a deep reservoir that could have fed mantle plumes beneath the  
440 Gondwana margin upon subduction cessation. Anomalous basement topography (0.5-1.2 km)  
441 centered beneath the West Antarctic margin and anomalously high Paleogene subsidence  
442 rates (total subsidence 0.5-0.9 km) of the Campbell Plateau greater than expected from rift  
443 basin models points to long-lived (>80 Ma) mantle upwelling below the Antarctic margin  
444 (Sutherland et al., 2010). It is suggested that subduction death allowed a broad low-velocity  
445 anomaly that is presently located at 400-1000 km depth to rise from 700-1500 km depth. This  
446 low-density anomaly must have had an original horizontal dimension of several thousands of  
447 kilometers and could be explained by an average temperature anomaly of 150-200°K  
448 (Sutherland et al., 2010). This large-scale low-density anomaly may be the source of the Late  
449 Cretaceous HIMU end member and collision of the Hikurangi Plateau with the Gondwana  
450 margin at ~110 may have triggered its upwelling (Sutherland et al., 2010). Although it was

451 speculated that this anomaly resulted from metasomatism of the mid-mantle by subducting  
452 slabs over the last 400 Ma, we note that this is not a sufficient amount of time to derive the  
453 high  $^{207}\text{Pb}/^{204}\text{Pb}$  isotopic signatures of the HIMU end member from a MORB source (1.0-3.2  
454 Ga) as discussed above. Therefore, this anomaly may ultimately tap a source in the lower  
455 mantle containing substantially older recycled ocean crust and/or SCLM.

456

#### 457 4.3 A model to explain Late Cretaceous HIMU Intraplate volcanism

458 We now present a model to explain the interaction of upwelling HIMU type mantle  
459 plume(s) with the Gondwana subduction zone jammed by the Hikurangi Plateau collision.  
460 Upwelling plume mantle beneath the Gondwana margin would be deflected upwards along  
461 the base of the slab until it arrived beneath the Hikurangi Plateau. Although it was no doubt  
462 difficult for magmas to ascend through the thickened plateau lithosphere, explaining why  
463 many show contamination by enriched (EM type) Hikurangi lithosphere, deep lithospheric  
464 fractures and faults formed during the collision of the plateau with the Gondwana margin at  
465 ~110-105 Ma (e.g. Davey et al., 2008; Barrett et al., 2018) could have facilitated the rise of  
466 the plume-derived magmas.

467 An important question is why extensive intraplate volcanism took place in Marlborough  
468 between 98-94 Ma, because the plume material would have likely been blocked from  
469 upwelling to shallow depths by the recently-subducted lithosphere beneath the Torlesse  
470 accretionary wedge. Interestingly, the Marlborough Igneous Province was located close to the  
471 subducted western margin of the Hikurangi Plateau. The west side of the Hikurangi Plateau is  
472 likely to have been bounded by a major transform fault/fracture zone (Mortimer et al., 2019).  
473 A sharp transition in thickness in the subducting crust along a tectonic lineament, such as a  
474 fracture zone, is a likely place for a slab tear to form, allowing plume mantle to flow into the  
475 mantle wedge. Formation of a slab tear along the western edge of the partially subducted

476 Hikurangi Plateau at ~100 Ma would have facilitated upwelling of HIMU plume material  
477 beneath the Marlborough area of the South Island and its interaction with enriched (Mt.  
478 Somers-type) mantle wedge, as well as forearc crust that is expected to have a similar  
479 composition.

480 In the Late Cretaceous, the Westland igneous province could have been located ~500 km  
481 SW of the Marlborough igneous province. The geochemical characteristics of the Westland  
482 igneous rocks are consistent with increased dilution of the HIMU end member as the plume  
483 material flowed through a progressively deeper slab tear below the arc/backarc region,  
484 resulting in greater contamination of the melts with enriched (EMORB type) mantle wedge.  
485 Interestingly, the southern progression of intraplate volcanism appears to have occurred along  
486 what in the future (at ~45 Ma) would become the Pacific-Australia plate boundary,  
487 suggesting that the Alpine Fault's location may have initially been influenced or even  
488 controlled by a slab tear at the western margin of the subducted portion of the Hikurangi  
489 Plateau (Reyners et al., 2011). The slab tear is likely to have propagated down dip with the  
490 plateau edge. As a result, hot plume mantle could have streamed through an elongate slab  
491 tear, thermally weakening the overlying lithosphere. Therefore, a precursor fault to the  
492 Alpine Fault may have formed in the Late Cretaceous (e.g., van der Meer et al., 2016).

493 Considering the similarity in isotopic composition, the East Chatham HIMU end member  
494 is likely to be derived from the same source (plume) that feed the Hikurangi, Marlborough  
495 and Westland volcanism. A SW propagating detachment of the subducting slab, possibly  
496 along an extension of the NE-SW-trending Western Wishbone Ridge, which has been  
497 interpreted to be a fracture zone or a major dextral strike-slip fault system (e.g. Mortimer et  
498 al., 2006; Barrett et al., 2018), or along the eastern boundary of the thick Hikurangi Plateau,  
499 could explain the opening of a slab window beneath the SE Chatham Rise margin. This  
500 window would have allowed plume material to upwell into and interact with the former

wedge mantle and the overlying continental crust. The opening of a slab window would have facilitated the upwelling of hotter, deeper asthenosphere, including hot plume mantle, to shallow depths, thermally eroding and weakening the overlying lithosphere and possibly triggering extension and rifting along the southern margin of the Chatham Rise and the Bounty Trough. Once significant thinning of the Gondwana continental lithosphere had occurred, including formation of the Bounty Trough (~90 Ma; Eagles et al., 2004), upwelling plume material could have melted by decompression to form the large intraplate seamounts, many being guyots (former ocean island volcanoes), and the extensive Cretaceous southern Chatham Island volcanism. The volcanism shortly preceded and was concurrent with seafloor spreading that initiated prior to 83 Ma in the mouth of the Bounty Trough (Davy, 2006).

Although the HIMU plume type volcanism along the rifted southeastern Chatham Rise margin is extensive, there is no evidence for the existence of seaward dipping reflectors or for a HIMU type flood basalt province. The lack of excess volcanism is not consistent with this being a volcanic rifted margin formed by interaction of a mantle plume head with the base of a continent. Instead we propose that the margin is a hybrid type that initially formed as non-volcanic margin and then became volcanically active in an intermediate to final stage of its evolution by interaction of “plumelets” (secondary plumes) from a HIMU type plume head stalled in the transition zone.

519

## 5. Conclusions

Four Late Cretaceous intraplate igneous provinces (Hikurangi, Marlborough, Westland and East Chatham) located on oceanic and diverse continental crust form crude binary mixing arrays between a common St. Helena-type HIMU component and depleted and enriched components located in the former Gondwana mantle wedge and the overlying lithosphere. A mantle plume has been imaged to the base of the lower mantle beneath the St. Helena

526 hotspot, providing evidence for a deep mantle plume source for St. Helena HIMU mantle. In  
527 contrast to most continental breakup events, there are no flood basalts associated with the  
528 final phase of Gondwana breakup separating Zealandia from Antarctica, as expected from a  
529 starting plume head (Richards et al., 1989), and no evidence for seaward-dipping reflectors at  
530 the rifted Chatham Rise margin. A possible source for the HIMU end member was the 700-  
531 1000 km deep, several thousand kilometers in size, mid-mantle low-density anomaly (with  
532 possible excess temperature of 150-200°K) postulated by Sutherland et al. (2010). The  
533 formation of one large plume or possibly multiple smaller plumes may have been triggered  
534 by the Hikurangi Plateau collision and subduction cessation, since for example subduction  
535 may have previously dragged such mantle downwards not allowing it to rise or detachment /  
536 change of subduction angle may have allowed the slab to destabilize the low-velocity  
537 anomaly allowing it to rise. Upwelling HIMU material from the mid mantle began to feed  
538 intraplate volcanism at ~100 Ma north and south of the Gondwana margin, lasting for ~30  
539 Ma. Rise of this plume material beneath the Gondwana continental margin was facilitated by  
540 the formation of a slab tear on the western side of the partially subducted Hikurangi Plateau  
541 (between ~98-69 Ma), followed by the opening of a slab window as a result of slab breakoff  
542 on the SE side of the subducted plateau (beginning at ~86 Ma). We propose that the  
543 upwelling hotter HIMU mantle from mid mantle depths and hotter upper mantle from below  
544 the slab upwelling through the slab window played a fundamental role in thermally  
545 weakening and extending the overlying lithosphere, first causing rifting in the Bounty Trough  
546 and Chatham Rise-Amundsen Sea sector (100-90 Ma) and then breakup and seafloor  
547 spreading along the SE margin of the Chatham Rise at ≤85 Ma, which propagated southwards  
548 to split the Campbell Plateau from West Antarctica. At ~65 Ma, there was a slight shift in the  
549 flavor of the HIMU end member composition towards less radiogenic  $^{207}\text{Pb}/^{204}\text{Pb}$  and more  
550 radiogenic  $^{143}\text{Nd}/^{144}\text{Nd}$ , as is the case for the HIMU end member in the Cenozoic Zealandia

lavas. The Cenozoic HIMU-type compositions are derived from a distinct source, either from SCLM metasomatized by Cretaceous plume activity or from a different plume source. In closing, we conclude that both Hikurangi Plateau collision and HIMU plume activity were essential in causing the separation of Zealandia from Gondwana.

## **Acknowledgements**

We thank the captains, crews and scientific parties of R/V SONNE cruises SO168 and SO246 for their excellent support on board. S. Hauff, K. Junge, and J. Sticklus at GEOMAR and U. Westernströer at Kiel University are gratefully acknowledged for analytical support and G. Wellschmidt for help with sample preparation. This study has been funded by the German Ministry of Education and Research (BMBF; grants 03G0246B and 03G0168A) and the German Research Foundation (DFG; grants HO18/12-1 and 2) are gratefully acknowledged for providing funding for this project. Additional funding has been provided by GNS Science, Canterbury University, the GEOMAR Helmholtz Center for Ocean Research Kiel and the Alfred-Wegener-Institut (AWI). CT was partly funded by the European Union's Horizon 2020 research and innovation program under the Marie Skłodowska-Curie grant agreement #79308.

## **Appendix. Supplementary material**

Supplementary material related to this article can be found on-line at <http://dx.doi.org/10.1016/j.epsl.....>

## **Figure Captions**

575 **Figure 1:** Bathymetric map (after Smith and Sandwell, 1997), showing Zealandia and the  
576 Hikurangi Plateau. Also shown are the four Cretaceous (99-69 Ma) intraplate igneous  
577 provinces (Hikurangi in yellow, Marlborough in green, Westland in blue and East Chatham  
578 in red), including sample locations within them, and the location of the Mt. Somers  
579 subduction-related volcanism (~98 Ma). The black line marks the plate boundary between the  
580 Pacific and Indo-Australian Plates. UFZ = Udintsev Fracture Zone; BFZ = Bollons Fracture  
581 Zone; PFZ = Pahemo Fracture Zone.

582  
583 **Figure 2:** Major element diagrams of MgO vs. a) SiO<sub>2</sub>, b) CaO, c) Al<sub>2</sub>O<sub>3</sub>, d) FeO<sup>t</sup> = total  
584 iron as FeO, e) TiO<sub>2</sub> and f) P<sub>2</sub>O<sub>5</sub>. Data sources: Eastern Chatham Rise = Mortimer et al.  
585 (2019), Homrighausen et al. (2018); Chatham Island Southern Volcanic rocks = Panter et al.  
586 (2006); Hikurangi Province = Hoernle et al. (2010); Osbourn Trough = Worthington et al.  
587 (2006); DSDP Site 595 = Mortimer et al. (2019); Marlborough = this study; McCoy-West et  
588 al. (2010); Mount Somers volcanic group = this study; Westland Province = this study; van  
589 der Meer et al. (2016), van der Meer et al. (2017); Cenozoic intraplate lavas = Hoernle et al.  
590 (2006); Timm et al. (2009); Timm et al. (2010).

591  
592 **Figure 3:** Diagram panels showing a) Nb/Y versus Zr/Ti after Pearce (1996), and b) Nb/Yb  
593 versus Th/Yb and c) Nb/Yb versus TiO<sub>2</sub>/Yb after Pearce (2008). Only samples with MgO>6  
594 wt.% are shown in c) to minimize the effect to magnetite-ilmenite fractionation. Data sources  
595 are as follows: Hikurangi Seamount Province = yellow circles (Hoernle et al., 2010);  
596 Marlborough Igneous Province = green triangles: Lookout Volcanics (this study; McCoy-  
597 West et al., 2010), Gridiron Volcanics (this study), Mandamus Igneous Complex (this study);  
598 Eastern Chatham Igneous Province: seamounts = red squares (this study; Homrighausen et  
599 al., 2018); Chatham Islands Southern Volcanic rocks (Panter et al., 2006); Westland Igneous



Province = blue hexagons (this study; van der Meer et al., 2016, van der Meer et al., 2017).  
Grey diamonds represent published data from Cenozoic Volcanic centers (age of <60 Ma)  
(sources as in figure 2).

**Figure 4:** Representative multi-element patterns for the freshest and most mafic samples  
with the most radiogenic Pb isotope ratios (most HIMU type composition): A) Hikurangi  
Seamount Province (Hoernle et al., 2010; filters used: MgO>3wt%. LOI<3wt%;  
 $^{206}\text{Pb}/^{204}\text{Pb}>19.95$ ), B) Westland Volcanic Province (filters used: MgO>5wt%; LOI<3.5wt%;  
 $^{206}\text{Pb}/^{204}\text{Pb}>19.19$ ), C) Marlborough Volcanic Province (filters used: MgO>4wt%;  
 $^{206}\text{Pb}/^{204}\text{Pb}>20.4$ ), D) Eastern Chatham Province (LOI<3wt%;  $^{206}\text{Pb}/^{204}\text{Pb}>19.6$ ), and E) Mt.  
Somers (MgO>5.5wt%). Data sources are as listed in Fig. 2 captions. Average N-MORB are  
after Sun and McDonough, (1989) and average St.Helena pattern are from data in Chaffey et  
al. (1989) and Hanyu et al. (2011).

**Figure 5:** Plots of initial A)  $^{206}\text{Pb}/^{204}\text{Pb}$  vs  $^{207}\text{Pb}/^{204}\text{Pb}$ , B)  $^{206}\text{Pb}/^{204}\text{Pb}$  vs  $^{143}\text{Nd}/^{144}\text{Nd}$  and C)  
 $^{206}\text{Pb}/^{204}\text{Pb}$  vs  $^{87}\text{Sr}/^{86}\text{Sr}$  isotope ratios for samples from this study and published data (see  
below), assuming an average age of 90 Ma for all Late Cretaceous samples. The St. Helena  
HIMU (Chaffey et al., 1989; Kawabata et al., 2011), Cook Austral HIMU (Kawabata et al.,  
2011; Hanyu et al., 2011) and Cenozoic Zealandia and Pacific MORB fields have been  
projected to 90 Ma, using the same parent/daughter ratios as employed by Homrighausen et  
al. (2018 and references therein). Sm = 6.5 ppm and Nd = 20 ppm were assumed for the  
DSDP 595  $^{143}\text{Nd}/^{144}\text{Nd}$  age correction. Mantle endmembers are from Zindler and Hart  
(1986). Data sources are: this study; McCoy-West et al. (2010); McCoy-West et al. (2016),  
Hoernle et al. (2010); Panter et al. (2006); Homrighausen et al. (2018); Mortimer et al.  
(2006); van der Meer et al. (2016); Hoernle et al. (2006); Timm et al. (2009) and Timm et al.

(2010). Late Cretaceous ocean crust, sampled at Bollons Gap (~77-85 Ma; Mortimer et al., 2019) and DSDP Site 595 (~84 Ma; Mortimer et al., 2019) has a depleted composition, pointing to a primarily depleted composition for the upper mantle in this area.

**Figure 6:** Conceptual model showing the evolution of the Zealandian continental margin during three different time periods (A = ~110-100 Ma; B = ~100-90 Ma and C ≤ 85 Ma). (A) At ~ 110 Ma, the Hikurangi Plateau collided with the Gondwana margin triggering rise of HIMU plume mantle to the base of the subducting Pacific Plate. (B) At ~100 Ma, upwelling plume material flows along the base of the subducting slab until it reaches the base of the Hikurangi Plateau, melting by decompression to form the Hikurangi Seamounts (yellow triangles). Mt. Somers volcanism (white triangle) takes place in the Gondwana forearc at ~98-96 Ma. A slab tear opened along the western, presumably fracture zone boundary, of the subducted portion of the Hikurangi Plateau. This tear allowed plume material to upwell to the base of the Gondwana lithosphere, also partially melting by decompression to form the Marlborough Igneous Province at 98-94 Ma and begin forming the Westland mafic igneous rocks (small blue triangles) beginning at ~92 Ma. (C) At ~85 Ma, a slab tear began at the eastern boundary of the Hikurangi Plateau (possibly at the Wishbone Fracture Zone) and propagated to the SW eventually resulting in slab detachment. The slab window allowed HIMU plume material to flood into the former Gondwana margin mantle wedge, triggering extension to form the Bounty Trough (~90-80 Ma), seafloor spreading (≤85 Ma) and formation of the East Chatham and SE Chatham Volcanic Province rocks (86-79 Ma).

## Supplementary Materials

Supplementary File 1: Analytical methods.

Supplementary Table 1: Major and trace element and Sr, Nd and Pb radiogenic isotope data.

Supplementary Table 2: Standard data for XRF and ICPMS analyses.

## References

Baker, J., Gamble, J., Graham, I.J. 1994. The age, geology and geochemistry of the Tapuaenuku Igneous Complex, Marlborough, New Zealand 37 (3), 249-268.

Barrett, R.S., Davy, B., Stern, T., Gohl, K., 2018. The strike-slip West Wishbone Ridge and the eastern margin of the Hikurangi Plateau. *Geochemistry Geophysics Geosystems*, 19, 1199-1216, doi:10.1002/2017GC007372.

Bradshaw, J. D. (1989) Cretaceous geotectonic patterns in the New Zealand Region. *Tectonics*, 8, 803–820.

Cabral, R.A., Jackson, M.G., Rose-Koga, E.F., Koga, K.T., Whitehouse, M.J., Antonelli, M.A., Farquhar, J., Day, J.M.D., Hauri, E.H. (2013) Anomalous sulphur isotopes in plume lavas reveal deep mantle storage of Archaean crust: *Nature*, v. 496, no. 7446, p. 490-493.

Chaffey, D.J., Cliff, R.A., Wilson, B.M. (1989) Characterization of the St Helena magma source. *Geological Society London Special Publications* 42, 257-276.

Condie, K.C. (2016) *Tectonic Settings*. In: *Earth as an Evolving Planetary System* (third edition). Academic Press, 43-88.

Davy, B., 2006. Bollons seamount and early New Zealand-Antarctic seafloor spreading. *Geochemistry, Geophys. Geosystems* 7. doi:10.1029/2005GC001191

676 Davy, B., Hoernle, K., Werner, R. 2008. Hikurangi Plateau: Crustal structure, rifted formation, and  
 677 Gondwana subduction history. *Geochemistry Geophysics Geosystems* 9 (7) Q07004,  
 678 doi:10.1029/2007GC001855  
 679  
 680 Davy, B. 2014. Rotation and offset of the Gondwana convergent margin in the New Zealand region  
 681 following Cretaceous jamming of Hikurangi Plateau large igneous province subduction. *Tectonics* 33,  
 682 1577-1595, doi:10.1002/2014TC003629.  
 683  
 684 Eagles, G., Gohl, K., Larter, R.D., 2004. High-resolution animated tectonic reconstruction of the  
 685 South Pacific and West Antarctic Margin. *Geochemistry Geophysics Geosystems* 5 (7),  
 686 DOI: 10.1029/2003GC000657.  
 687  
 688 French, S.W., Romanowicz, B., 2015. Broad plumes rooted at the base of the Earth's  
 689 mantle beneath major hotspots. *Nature* 525 (7567), 95–99.  
 690  
 691 Geoffroy, L. (2005) Volcanic passive margins. *C. R. Geoscience* 337, 1395–1408.  
 692  
 693 Gohl, K., Werner, R. (2016), the expedition SO246 of the Research Vessel SONNE to the Chatham  
 694 Rise in 2016. *Berichte zur Polar- und Meeresforschung = Reports on polar and marine research*,  
 695 Bremerhaven, Alfred Wegener Institute for Polar and Marine Research, 698, p. 158.  
 696  
 697 Golowin R, Portnyagin M, Hoernle K, Hauff F, Gurenko A, Garbe-Schönberg D, Werner R and  
 698 Turner, S (2017) Boninite-like intraplate magmas from Manihiki Plateau require ultra-depleted and  
 699 enriched source components. *Nature Communication* 8: 14322. DOI 10.1038/ncomms14322.  
 700  
 701 Hanyu, T., Tatsumi, Y., Senda, R., Miyazaki, T., Chang, Q., Hirahara, Y., Takahashi, T., Kawabata,  
 702 H., Suzuki, K., Kimura, J.-I. (2011) Geochemical characteristics and origin of the HIMU reservoir: A

703 possible mantle plume source in the lower mantle, *Geochem. Geophys. Geosyst.*, 12, Q0AC09,  
 704 doi:10.1029/2010GC003252.  
 705  
 706 Hart, S.R., Blusztajn, J., LeMasurier, W.E., Rex, D.C., 1997. Hobbs Coast Cenozoic volcanism:  
 707 implications for the West Antarctic rift system. *Chemical Geology*, 139, 223–248.  
 708  
 709 Hochmuth, K., Gohl, K., Uenzelmann-Neben, G., 2015. Playing jigsaw with Large Igneous Provinces  
 710 – A plate tectonic reconstruction of Ontong Java Nui, West Pacific. *Geochemistry, Geophysics,*  
 711 *Geosystems*, 16, 3789–3807, doi:10.1002/2015GC006036.  
 712  
 713 Hoernle, K., White, J. D. L., van den Bogaard, P., Hauff, F., Coombs, D. S., Werner, R., Timm, C.,  
 714 Garbe-Schoenberg, D., Reay, A. & Cooper, A., 2006. Cenozoic intraplate volcanism on New Zealand:  
 715 Upwelling induced by lithospheric removal. *Earth and Planetary Science Letters* 248, 335–352.  
 716  
 717 Hoernle, K., Hauff, F., Bogaard, Pvd., Werner, R., Mortimer, N., Geldmacher, J., Garbe-Schoenberg,  
 718 D. & Davy, B., 2010. Age and geochemistry of volcanic rocks from the Hikurangi and Manihiki  
 719 oceanic Plateaus. *Geochimica et Cosmochimica Acta* 74, 7196–7219, doi:10.1016/j.gca.2010.09.030.  
 720  
 721 Hofmann, A.W. (1997) Mantle geochemistry: The message from oceanic volcanism. *Nature*  
 722 385(6613), 219–229.  
 723  
 724 Hofmann, A.W., White, W.M., 1982. Mantle plumes from ancient oceanic crust. *Earth*  
 725 *Planet. Sci. Lett.* 57 (2), 421–436.  
 726  
 727 Homrighausen, S., Hoernle, K., Hauff, F., Geldmacher, J., van den Bogaard, P., Garbe-Schoenberg,  
 728 D., 2018. Global distribution of the HIMU end member: Formation through Archean plume-lid  
 729 tectonics. *Earth Science Reviews* 182, 85–101.  
 730

Formatted: English (United States)

731 Kimura J-I, Gill, J.B., Skora, S., van Keken, P.E., Kawabata, H. (2016) Origin of geochemical mantle  
 732 components: Role of subduction filter. *Geochem. Geophys. Geosyst.* 17, 8, 3289-3325.  
 733  
 734 Luyendyk, B.R. 1995. Hypothesis for Cretaceous rifting of east Gondwana caused by subduction slab  
 735 capture. *Geology* 23 (4), 373-376.  
 736  
 737 McCoy-West, A., Baker, J., Faure, K., Wysoczanski, R., 2010. Petrogenesis and Origins of Mid-  
 738 Cretaceous Continental Intraplate Volcanism in Marlborough, New Zealand: Implications for the  
 739 Long-lived HIMU Magmatic Mega-province of the SW Pacific. *Journal of Petrology* 51 (10), 2003-  
 740 2045.  
 741  
 742 McCoy-West, A., Bennet, V.C., Amelin, Y., 2016. Rapid Cenozoic ingrowth of isotopic signatures  
 743 simulating “HIMU” in ancient lithospheric mantle: Distinguishing source from process. *Geochimica*  
 744 *et Cosmochimica Acta* 187, 79-101.  
 745  
 746 Menzies, M.A., Klemperer, S.L., Ebinger, C.J., Baker, J. (2002) Characteristics of volcanic rifted  
 747 margins, in Menzies, M.A., Klemperer, S.L., Ebinger, C.J., Baker, J., eds., *Volcanic Rifted Margins:*  
 748 *Boulder, Colorado, Geological Society of America Special Paper* 362, p. 1–14.  
 749  
 750 Montelli, R., Nolet, G., Dahlen, R.A., Masters, G., 2006. A catalogue of deep mantle plumes: New  
 751 results from finite frequency tomography. *Geochemistry Geophysics Geosystems* 7(11), Q11007,  
 752 doi:10.1029/2006GC001248.  
 753  
 754 Mortimer, N., Hoernle, K., Hauff, F., Palin, M., Dunlap, W.J., Werner, R., Faure, K. 2006. New  
 755 constraints on the age and evolution of the Wishbone Ridge, southwest Pacific Cretaceous  
 756 microplates, and Zealandia–West Antarctica breakup. *Geology* 34 (3) 185-188, doi:  
 757 10.1130/G22168.1  
 758

759 Mortimer, N, Campbell, H.J., Tulloch, A.J., King, P.R., Stagpoole, V.M., Wood, R.A., Rattenbury,  
760 M.S., Sutherland, R., Adams, C.J., Collot, J., Seton, M. 2017. Zealandia: Earth's Hidden Continent.  
761 GSA Today 27 (3), 27-35  
762  
763 Mortimer, N., van den Bogaard, P., Hoernle, K., Timm, C., Gans, P.B., Werner, R. Riefstahl, F.,  
764 2019. Late Cretaceous oceanic plate reorganisation in the SW Pacific-Zealandia region. *Gondwana*  
765 *Research* 65, 31-42.  
766  
767 Nebel, O., Arculus, R.J., van Westrenen, W., Woodhead, J.D., Jenner, F.E., Nebel-Jacobsen, Y.J.,  
768 Wille, M., Eggins, S.M., 2013. Coupled Hf–Nd–Pb isotope co-variations of HIMU oceanic island  
769 basalts from Mangaia, Cook-Austral islands, suggest an Archean source component in the mantle  
770 transition zone. *Geochim. Cosmochim. Acta* 112, 87–101.  
771  
772 Panter, K.S., Hart, R.S., Kyle, P.R., Blusztajn, J., Wilch, T., (2000) Geochemistry of Late Cenozoic  
773 basalts from the Crary Mountains: characterisation of mantle sources in Marie Byrd Land, Antarctica.  
774 *Chemical Geology*, 165, 215–241.  
775  
776 Panter, K. S., Blusztajn, J., Hart, S., Kyle, P., Esser, R. & McIntosh, W. (2006). The origin of HIMU  
777 in the SW Pacific: evidence from intraplate volcanism in southern New Zealand and subantarctic  
778 islands. *Journal of Petrology* 47, 1673–1704.  
779  
780 Pearce, J.A., 2008. Geochemical fingerprinting of oceanic basalts with applications to ophiolite  
781 classification and the search of Archean oceanic crust. *Lithos* 100, 14-48.  
782  
783 Reyners, M., Eberhart-Phillips, D. & Bannister, S. Tracking repeated subduction of the Hikurangi  
784 Plateau beneath New Zealand. *Earth and Planetary Science Letters* 311 (1-2), 165-171 (2011)  
785

786   Reyners, M., Eberhart-Phillips, D., Upton, P. Gubbins, D., 2017. Three-dimensional imaging of  
787   impact of a large igneous province with a subduction zone. *Earth and Planetary Science Letters* 460,  
788   143-151.  
789  
790   Richards, M.A., Duncan, R.A., Courtillot, V.E. (1989) Flood basalts and hot-spot tracks: plume heads  
791   and tails. *Science* 246, 103-107, doi:10.1126/science.246.4926.103.  
792  
793   Scott, J.M., Waight, T.E., Van der Meer, Q.H.A., Palin, J.M., Cooper, A.F., Münker, C., 2014.  
794   Metasomatized ancient lithospheric mantle beneath the young Zealandia microcontinent and its role in  
795   HIMU-like intraplate magmatism *Geochemistry, Geophysics, Geosystems* 15 (9), 3477-3501  
796  
797   Sleep, N.H. (1971) Thermal effects of the formation of Atlantic continental margins by continental  
798   breakup. *Geophys. J. R. Astron. Soc.*, 24, 325-350.  
799  
800   Smith, W.H.F., Sandwell, D.T., 1997. Global Sea Floor Topography from Satellite Altimetry and  
801   Ship Depth Soundings. *Science* 277, 1956-1962.  
802  
803   Storey, B.C., Leat, P.T., Weaver, S.D., Pankhurst, R.J., Bradshaw, J.D., Kelley, S. 1999. Mantle  
804   plumes and Antarctica-New Zealand rifting: evidence from mid-Cretaceous mafic dykes. *Journal of*  
805   *the Geological Society, London* 156, 659-671.  
806  
807   Sutherland, R., Spasojevic, S., Gurnis, M. 2010. Mantle upwelling after Gondwana subduction death  
808   explains anomalous topography and subsidence histories of eastern New Zealand and West  
809   Antarctica. *Geology* 38, 155-158, doi: 10.1130/G30613.1  
810  
811   Tappenden, V. (2003). Magmatic response to the evolving New Zealand Margin of Gondwana during  
812   the Mid-Late Cretaceous. Department of Geological Sciences Christchurch, University of Canterbury.  
813   PhD, 250 pp.



814

815 Taylor, B., 2006. The single largest oceanic plateau: Ontong Java–Manihiki–Hikurangi. *Earth Planet.*

816 *Sci. Lett.* 241 (3–4), 372–380.

817

818 Timm, C., Hoernle, K., van den Bogaard, P., Bindeman, I., Weaver, S. (2009). Geochemical evolution

819 of intraplate volcanism at Banks Peninsula, New Zealand: Interaction between asthenospheric and

820 lithospheric melts. *Journal of Petrology* 50, 1–35.

821

822 Timm, C., Hoernle, K., Werner, R., Hauff, F., van den Bogaard, P., White, J., Mortimer, N., Garbe-

823 Schoenberg, D., 2010. Temporal and geochemical evolution of the Cenozoic intraplate volcanism of

824 Zealandia. *Earth-Science Reviews* 98, 38–64.

825

826 Timm, C., Hoernle, K., Werner, R., Hauff, F., van den Bogaard, P., Michael, P., Coffin, M.F.,

827 Koppers, A. (2011). Age and geochemistry of the oceanic Manihiki Plateau, SW Pacific: New

828 evidence for a plume origin. *Earth and Planetary Science Letters* 304, 135–146.

829

830 Todt, W., Cliff, R.A., Hanser, A., Hofmann, A.W., 1996.  $^{202}\text{Pb} + ^{205}\text{Pb}$  double spike for lead isotopic

831 analyses. In: A Basu and S Hart (eds.) *Earth Processes: Reading the Isotopic Code: Geophysical*

832 *Monograph* vol 95

833

834 Tulloch, A.J., Ramezani, J., Mortimer, N., Mortensen, J., van den Bogaard, P., Maas, R. 2009.

835 Cretaceous felsic volcanism in New Zealand and Lord Howe Rise (Zealandia) as a precursor to final

836 Gondwana break-up. *Geological Society, London, Special Publication* 321, 89–118.

837

838 Tulloch, A.J., Mortimer, N., Ireland, T.R., Waight, T.E., Maas, R., Palin, M., Sahoo, T., Seebeck, H.,

839 Sagar, M., Barrier, A., Turnbull, R., 2019. Reconnaissance basement geology and tectonics of South

840 Zealandia. *Tectonics* 1–36. doi:10.1029/2018TC005116

841

842 Van der Meer, Q., Storey, B., Scott, J.M., Waight, T. 2016. Abrupt spatial and geochemical changes  
843 in lamprophyre magmatism related to Gondwana fragmentation prior, during and after opening of the  
844 Tasman Sea. *Gondwana Research* 36, 142-156.

845

846 Van der Meer, Q.H.A., Waight, T.E., Scott, J.M., Münker, C., 2017. Variable sources for Cretaceous  
847 to recent HIMU and HIMU-like intraplate magmatism in New Zealand. *Earth and Planetary Science*  
848 *Letters* 469, 27-41

849 Van der Meer, Q.H.A., Waight, T., Tulloch, A., Whitehouse, M., Andersen, T. 2018. Magmatic  
850 Evolution during the Cretaceous Transition from Subduction to Continental Break-up of the Eastern  
851 Gondwana Margin (New Zealand) documented by *in-situ* Zircon O–Hf Isotopes and Bulk-rock Sr–Nd  
852 Isotopes. *Journal of Petrology* 59, 849-880.

853 Weaver, S.D., Storey, B.C., Pankhurst, R.J., Mukasa, S.B., DiVenere, V.J., and Bradshaw,  
854 J.D., 1994, Antarctica–New Zealand rifting and Marie Byrd Land lithospheric magmatism linked to  
855 ridge subduction and mantle plume activity: *Geology*, v. 22, p. 811–814.

856

857 Worthington, T., Hekinian, R., Stoffers, P., Kuhn, T., Hauff, F. (2006). Osbourne Trough: Structure,  
858 geochemistry and implications of a mid-Cretaceous paleosspreading ridge in the South Pacific. *Earth*  
859 *and Planetary Science Letters* 245, 685-701.

860

861 Zindler, A., Hart, S., 1986. Chemical Geodynamics. *Annual Reviews of Earth and Planetary Science*  
862 14, 493-571.

Figure 1  
Click here to download Figure: Fig1\_ZealandiaMap\_Hoernle\_lowRes.pdf

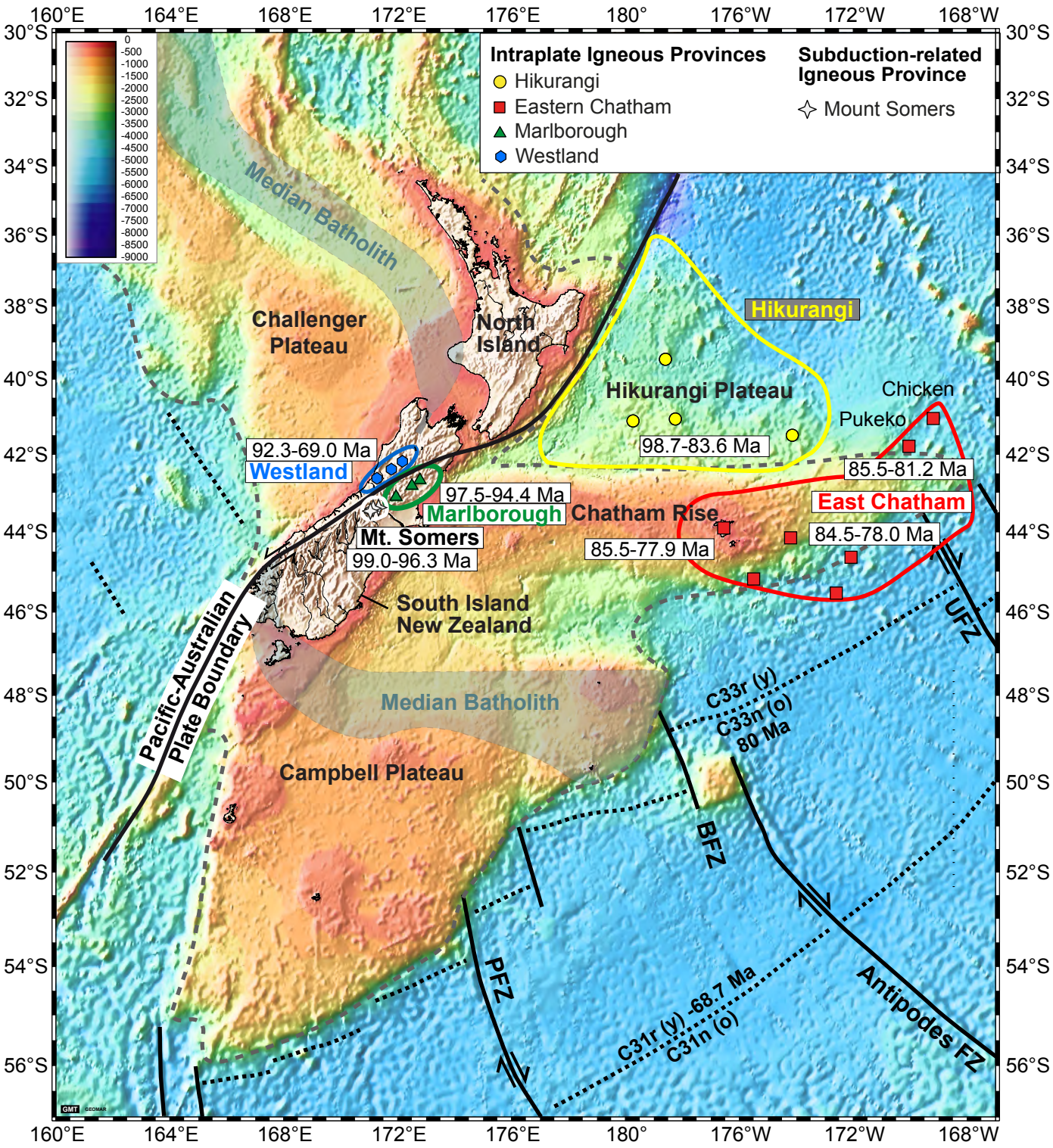


Figure 2  
[Click here to download Figure: Fig2\\_Majors\\_Hoernle.pdf](#)

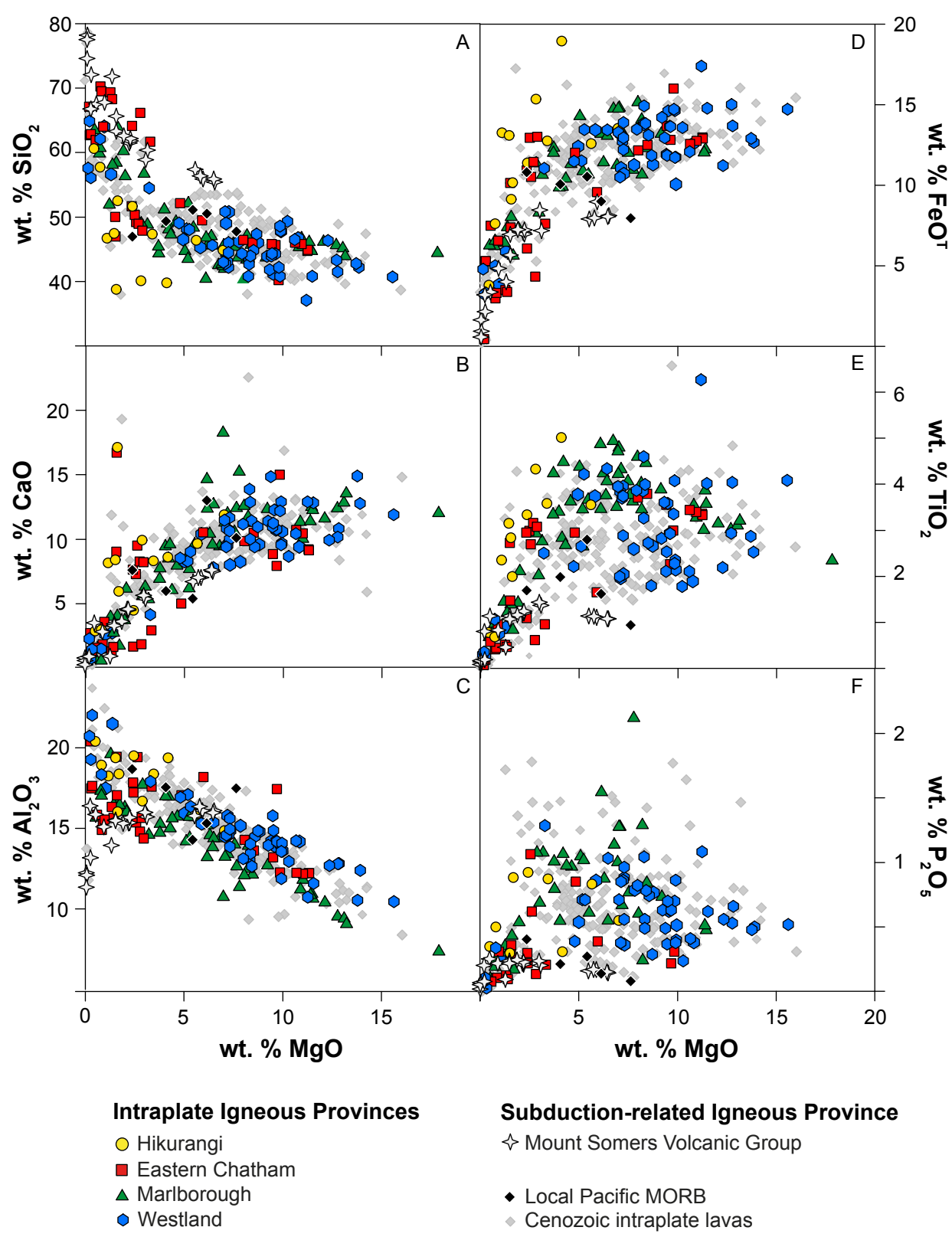




Figure 3  
Click here to download Figure: Fig3\_RockClass\_Hoernle.pdf

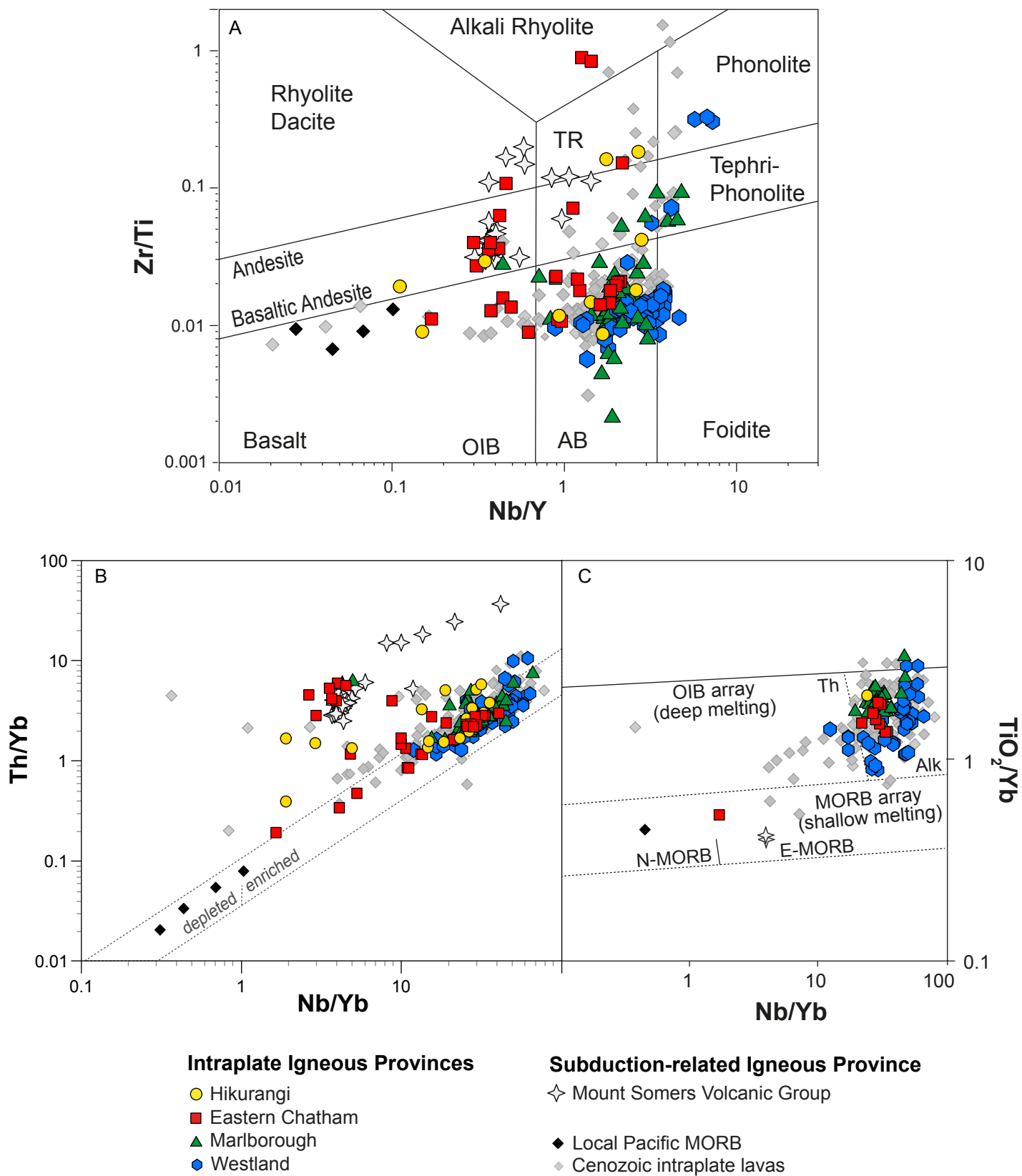


Figure 4  
[Click here to download Figure: Fig4\\_IncompatibleElements\\_Hoernle.pdf](#)

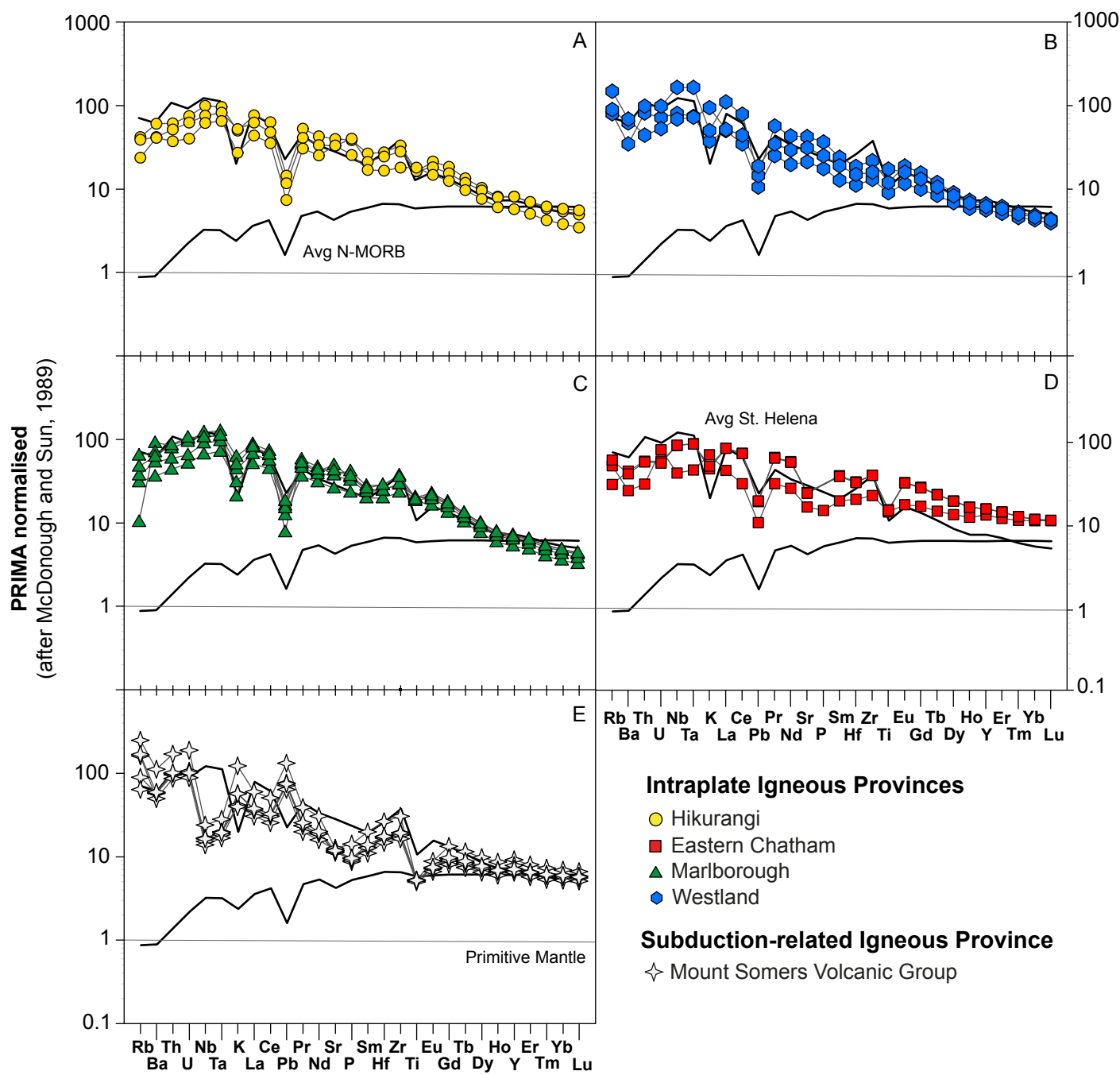
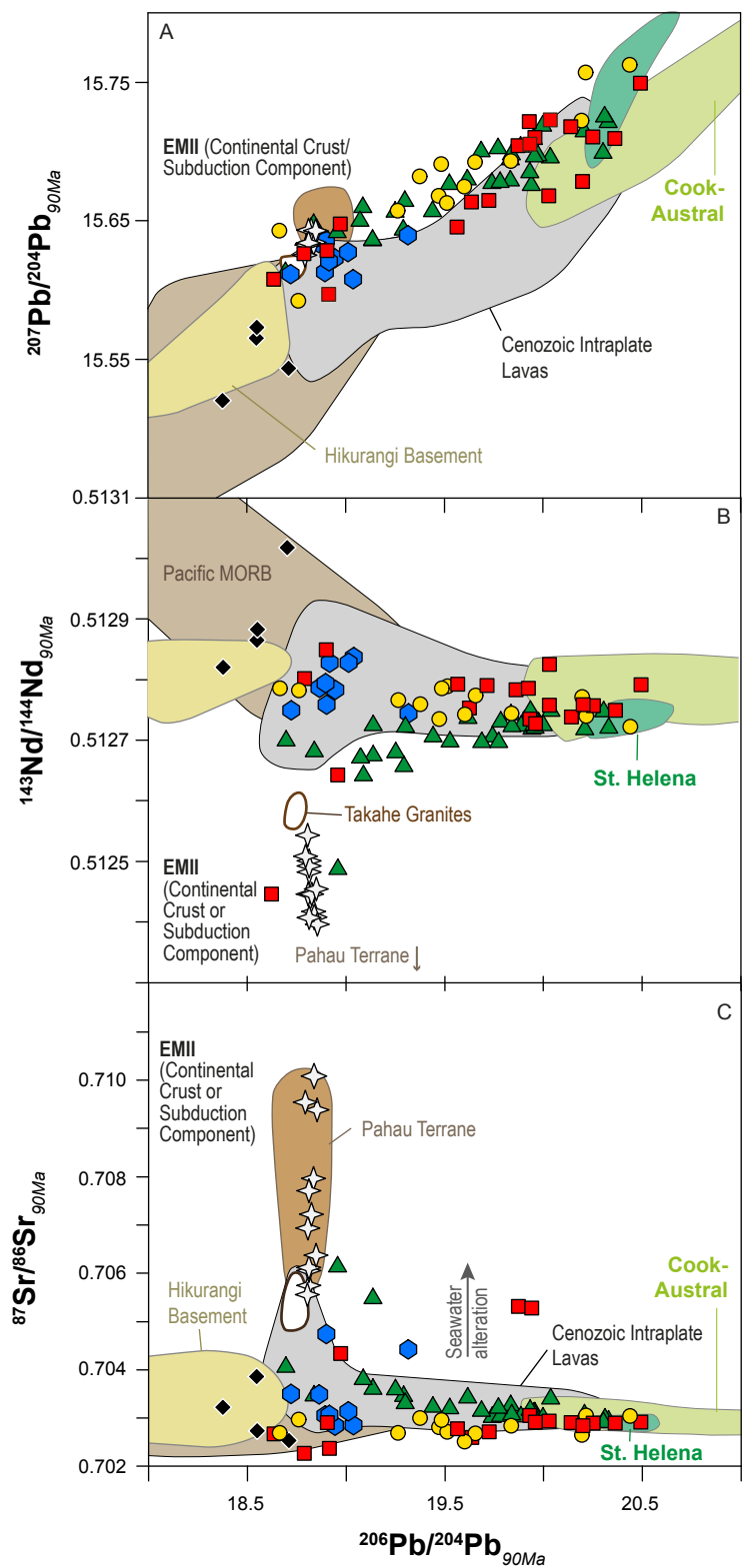


Figure 5  
Click here to download Figure: Fig5\_Isotopes\_Hoernle.pdf



- | Intraplate Igneous Provinces                       | Subduction-related Igneous Province                             |
|--|---|
| <span style="color: yellow;">●</span> Hikurangi    | <span style="color: grey;">☆</span> Mount Somers Volcanic Group |
| <span style="color: red;">■</span> Eastern Chatham | <span style="color: black;">◆</span> Local Pacific MORB         |
| <span style="color: green;">▲</span> Marlborough   |   |
| <span style="color: blue;">⬢</span> Westland       |   |

Figure 6  
[Click here to download Figure: Fig6\\_Model3D\\_Hoernle.pdf](#)

